Tunable Nonreciprocal Response of $KTaO_3$-Based Two-Terminal Device

Hui Zhang, Dongyao Zheng, Yinan Xiao, Daming Tian, Weijian Qi, Fengxia Hu, Baogen Shen, Jirong Sun, and Weisheng Zhao, *Fellow, IEEE*

***Abstract*—Two-dimensional electron gases (2DEGs) at oxide interfaces possess many interesting physical properties. Particularly, when the time reversal symmetry is broken, they display a large unidirectional magnetoresistance, which is essential for exploiting two-terminal devices based on such a nonreciprocal response. Here we report a nonreciprocal charge transport behavior in conductive 2DEG at the $LaAlO_3/KTaO_3$ interface, and the nonreciprocal coefficient γ of up to ~6.8 × $10^{-10} A^{-1}T^{-1}cm^2$ is obtained. Remarkably, the nonreciprocal response is highly tunable by applying gate voltages in a field-effect device. Our work illustrates that $KTaO_3$-based 2DEG is an outstanding platform for the development of multifunctional two-terminal devices and may pave a route for future gate voltage tunable rectification devices.**

***Index Terms*—Nonreciprocal response, Rashba spin-orbit coupling, two-dimensional electron gases, two-terminal device, gating effect.**

I. Introduction

NONRECIPROCAL response, i.e., current-direction dependent resistance, is sensitive to the broken inversion symmetry of the electronic state [1], which sparks a surge of interest in realizing two-terminal rectification, memory, and logic devices [2], [3], [4]. Nonreciprocal response has been observed in different materials with inversion symmetry breaking, such as noncentrosymmetric system [5], [6], [7], low-dimensional materials [8], [9], [10] and topological insulator [11], [12], [13]. Among them, two-dimensional electron gas (2DEG) at the interface between two insulating oxides has attracted extensive attention due to large Rashba spin-orbit coupling (SOC) [14], [15], [16], [17]. Strong nonreciprocal response has been observed in $SrTiO_3$(STO)-based 2EDGs [18] and the bilinear magnetoresistance (BMR) is highly anisotropic [19], which is a characteristic of unidirectional magnetoresistance yielded via nonreciprocity [20], [21]. More importantly, the strength of Rashba SOC and the carrier density can be effectively tuned by the gate voltage [22], [23], [24]. Gate-tunable nonreciprocal charge transport has been achieved at the $LaAlO_3/SrTiO_3$(LAO/STO) interfaces. In particular, compared to the 3d transition metal oxide STO, $KTaO_3$ (KTO) possesses a high permittivity similar to STO, while has a stronger Rashba SOC because Ta is a 5d element and heavier than Ti [25], [26]. Indeed, the research on the unidirectional magnetoresistance of 2DEG at the Al/KTO interface indicates that the Rashba coefficient extracted from the BMR analysis is significantly higher than that found in STO-based 2DEGs [8]. Unfortunately, so far works on the gating effect of nonreciprocal response of KTO-based 2DEGs are scarce.

Here we present a systematic investigation on the nonreciprocal response of 2DEG at the LAO/KTO interface, which is clearly verified by BMR effect. The current-induced Rashba field (H_R) is determined by quantitative analysis of the angle-dependent transport, and we found that the magnitude of the nonreciprocal response is strongly dependent on the carrier density. Furthermore, we fabricated a field-effect device based on gating effect and realized the modulation of carrier density thus effectively tuning the nonreciprocal response. Notably, the giant tunability of the nonreciprocal response at the LAO/KTO interfaces provides a possibility to achieve electric field tunable two-terminal devices.

II. Device Fabrication and Nonrecripical Response

Using standard optical lithography and lift off techniques, Hall bars (10 μm in width and 60 μm in length) were pre- patterned onto the (001)-oriented single crystalline KTO substrates by a hard-mask method. As shown in Fig.1(d), a 100-nm AlO_x film was used as a hard mask (dark region), prepared by pulsed laser deposition (PLD) at room temperature with a fixed oxygen pressure of 1 Pa. Next, the 2DEGs were fabricated by growing 10-nm-thick LAO films by PLD at 700 °C. The oxygen pressures during the growth of two devices are 1×10^{-4} Pa for device A and 5×10^{-4} Pa for device B, respectively. After growth of LAO, only the active Hall bar area (light region in Fig.1(d)) is conducting. Note that the LAO films are amorphous, due to the large lattice mismatch between LAO (0.379 nm) and KTO (0.399 nm) [24], [27]. Fig.1(a) presents the temperature dependence of the sheet resistance (R_S) of the 2DEGs for device A and

Manuscript received 18 December 2023; revised 12 January 2024; accepted 13 January 2024. Date of publication 17 January 2024; date of current version 27 February 2024. This work was supported in part by the Open Research Fund of the Songshan Lake Materials Laboratory under Grant 2022SLABFN23; and in part by the National Natural Science Foundation of China under Grant 12004022, Grant 11934016, and Grant 51972335. The review of this letter was arranged by Editor A. I. Khan. *(Corresponding authors: Hui Zhang; Weisheng Zhao.)*

Hui Zhang, Dongyao Zheng, Yinan Xiao, Daming Tian, Weijian Qi, and Weisheng Zhao are with the School of Integrated Circuit Science and Engineering, Beihang University, Beijing 100191, China (e-mail: huizh@buaa.edu.cn; wszhao@buaa.edu.cn).

Fengxia Hu, Baogen Shen, and Jirong Sun are with the Beijing National Laboratory for Condensed Matter Physics, Institute of Physics, Chinese Academy of Sciences, Beijing 100190, China.

Color versions of one or more figures in this letter are available at https://doi.org/10.1109/LED.2024.3355240.

Digital Object Identifier 10.1109/LED.2024.3355240

0741-3106 © 2024 IEEE. Personal use is permitted, but republication/redistribution requires IEEE permission.
See https://www.ieee.org/publications/rights/index.html for more information.

Authorized licensed use limited to: INSTITUTE OF PHYSICS CAS. Downloaded on June 24,2024 at 03:10:16 UTC from IEEE Xplore. Restrictions apply.

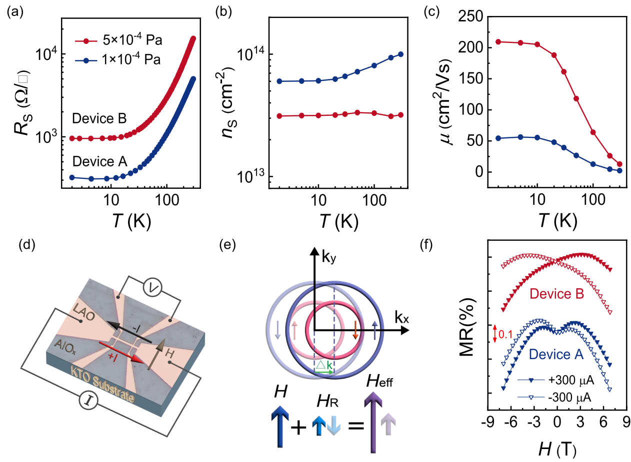

Fig. 1. (a-c) Temperature dependence of sheet resistance (a), carrier density (b) and Hall mobility (c). (d) Photograph of a typical Hall bar device. (e) Fermi contours of a 2DEG system. (d) In plane MR curves.

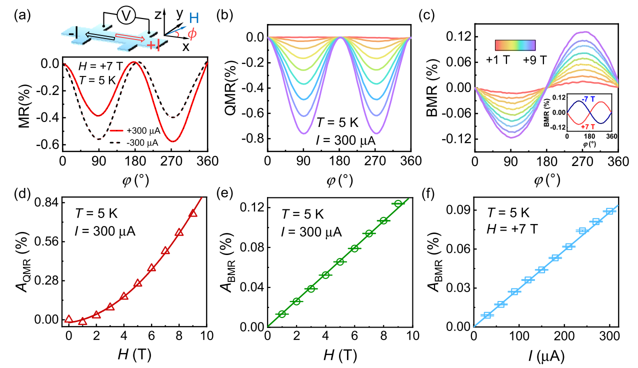

Fig. 2. (a) MR curves measured under an in-plane rotating magnetic field for both direction of currents for device A. The plot above is a sketch for experimental setup. (b-c) Angle dependence of the QMR (b) and the BMR (c). The inset of (c) shows nonreciprocal response by reversing the sign of the magnetic field (±7 T). (d-e) Magnetic field dependence of the A_{QMR} (d) and A_{BMR} (e). (f) A_{BMR} as a function of the applied current.

device B, both of which are well metallic. The carrier density (n_S) and the corresponding Hall mobility (μ), deduced from the Hall effect, as functions of temperature are displayed in Figs.1(b) and 1(c). Noted that the temperature dependence of sheet resistance and Hall effect were measured by applying a small current of 1 μA. We found the overall R_S-T curve of device B displays an upward shift. In addition, the n_S of device B ($\sim 3 \times 10^{13}$ cm^{-2}) is only the half of that of device A ($\sim 6 \times 10^{13}$ cm^{-2}) at $T = 2$ K. While the Hall mobility of device B is about 200 cm^2/Vs at $T = 2$ K, which is greater by a factor of 4 than that of device A. The decrease of the n_S as the growth oxygen pressure increases indicates that the electron doping by oxygen vacancies plays an important role in forming the 2DEGs.

As shown in Fig.1(e), due to the Rashba effect the application of a current will induce the shift Δk of the Fermi contour and the resulting spin accumulation can be described by a current-induced Rashba field (H_R), which is constrained in the film plane and perpendicular to the direction of applied current. Depending on the direction of the current, H_R is added to (or subtracted from) external magnetic field (H) perpendicular to applied current, resulting in an effective magnetic field $H_{eff} = H \pm H_R$.Via this mechanism, nonreciprocal resistive responses can be achieved by reversing either the sign of the magnetic field or the polarity of the current. Fig.1(f) shows the in-plane magnetoresistance (MR), defined as MR=$[R_{xx}(H, I) - R_{xx}(0, I)]/R_{xx}(0, I)$, where H is perpendicular to the current direction in the film plane. The measurements were done with an applied current $I = \pm 300$ μA at $T = 5$ K. We used pulsed currents with a duration of 80 ms and an interval of 4000 ms to effectively eliminate the influence of joule heating. The extremely asymmetric MR curves and significant differences between MR under $+I$ and $-I$ clearly exhibit the nonreciprocal charge transport in the 2DEGs at the LAO/KTO interfaces. In addition, the nonreciprocal response of KTO-based 2DEG with low carrier density is significantly greater.

III. Bilinear Magnetoresistance of KTO-Based Device

The angle-dependent transport experiments were further carried out. Measurement setup is sketched in Fig.2(a), where current is applied along x axis and φ denotes the angle between magnetic field and the x axis. MR curves measured under a rotating in-plane external magnetic field at 5 K for device A are shown in Fig.2(a), where H is fixed to +7 T and $I = \pm 300$ μA. When the applied field is perpendicular to the current ($\varphi = 90°$ or 270°), the MR is minimal and a pronounced asymmetry between $\varphi = 90°$ and 270° is observed. When reversing the polarity of the current, this asymmetry of the two minima reverses. We further extract the H-quadratic (symmetric) and bilinear (asymmetric) components of MR following the definitions: QMR=$[\mathrm{MR}(H, +I)+\mathrm{MR}(H, -I)]/2$ and BMR=$[\mathrm{MR}(H, +I)-\mathrm{MR}(H, -I)]/2$ [18]. The angle dependence of extracted QMR and BMR at varied magnetic field, ranging from +1 to +9 T, are shown in Figs.2(b) and 2(c), respectively. Notably, the inset of Fig.2(c) shows BMR changes sign when reversing the sign of the magnetic field (±7 T), verifying the nonreciprocal resistive responses can also be achieved by reversing the magnetic field. By fitting the data to QMR= $A_{QMR}\cos(2\varphi)$ and BMR= $A_{BMR}\sin\varphi$, the amplitudes of QMR and BMR can be further obtained. As plotted in Fig.2(d), A_{QMR} shows a quadratic relationship with H, where the red solid line is a quadratic fitting curve. In Fig.2(e), A_{BMR} strongly increases with H and clearly scales linearly with H. Furthermore, the angular-dependent MR is also measured by varying the applied current at a fixed magnetic field $H = +7$ T. A_{BMR} also shows a linear dependence of I, as displayed in Fig.2(f). Remarkably, the amplitude of asymmetric contribution A_{BMR} is linear with both H and I. Thus BMR effect unambiguously verifies the nonreciprocal charge transport. Then, the nonreciprocal coefficient γ is calculated by $\gamma = A_{BMR}/HJ$, where $J = I/S$ is the current density and S is the cross-sectional area of the Hall bar. The values of γ are as high as $\sim 4.2 \times 10^{-10}$A^{-1}T^{-1}cm^2 for device A and $\sim 6.8 \times 10^{-10}$A^{-1}T^{-1}cm^2 for device B, which are one order of magnitude larger than that of other typical systems, such as α-GeTe ($\gamma \sim 1 \times 10^{-11}$A^{-1}T^{-1}cm^2) [2] and Bi_2Se_3 ($\gamma \sim 2 \times 10^{-11}$A^{-1}T^{-1}cm^2) [11].

IV. Electric Field Control of RASHBA Field

The resistance R_{xx} is jointly determined by external magnetic field H and current-induced Rashba field H_R(Fig.1(e)), thus we can get direct information on H_R by analyzing anisotropic MR. Due to device B possesses larger nonreciprocal coefficient and stronger nonreciprocal response,

Authorized licensed use limited to: INSTITUTE OF PHYSICS CAS. Downloaded on June 24,2024 at 03:10:16 UTC from IEEE Xplore. Restrictions apply.

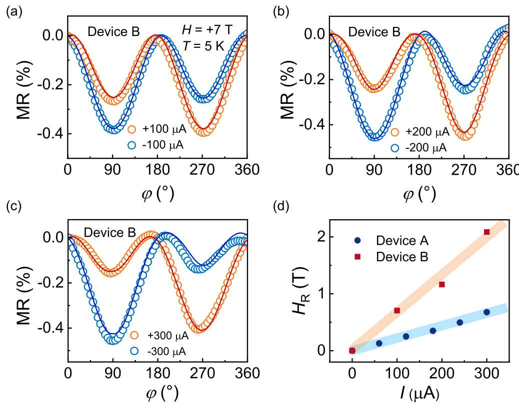

Fig. 3. (a-c) Magnetoresistance (symbols) measured with the applied current $I = \pm$ 100 μA (a), $\pm$200 μA (b) and $\pm$300 μA (c). (d) The deduced Rashba field as a function of electric current.

we focused on the representative device B to further investigate the current-induced Rashba field. Figs.3 (a-c) illustrate the angle dependence of MR for the device B with $H = +7$ T at 5 K by varying the applied current from 100 to 300 μA. It is clear that with increasing applied current values, the asymmetry between $\varphi = 90°$ and $\varphi = 270°$ of MR increases. Based on the equations [28]:

$$R = a_0 + a_1 H_{\rm eff}^2 \cos^2(\frac{\pi}{2} - \phi - \alpha) + a_2 H_{\rm eff}^2 \cos^4(\frac{\pi}{2} - \phi - \alpha) \quad (1)$$

$$H_{\rm eff}^2 = H^2 + H_{\rm R}^2 + 2HH_{\rm R}\sin\phi \quad (2)$$

$$\alpha = \arctan\frac{H_{\rm R}\cos\phi}{H + H_{\rm R}\sin\phi} \quad (3)$$

the experimental results have been well reproduced (the symbols are experiment data and the solid lines are the results of curve fitting) adopting appropriate fitting parameters a_0, a_1, a_2 and $H_{\rm R}$. Fig.3(d) summarizes the deduced $H_{\rm R}$ determined by data fitting for device A and device B, as a function of electric current. The $H_{\rm R}$ values of both devices scale linearly with increasing I. However, the current-induced $H_{\rm R}$ of device B is much larger than that of device A. Obviously, the lower $n_{\rm S}$ is, the larger $H_{\rm R}$ is, which is consistent with the result in Fig.1(f), suggesting that the band structure near the Fermi surface of 2DEG with lower $n_{\rm S}$ may have greater spin splitting.

As the carrier density of 2DEG at the LAO/KTO interface is gate-controllable, a further tuning of the nonreciprocal response can be achieved by applying a back-gate voltage $V_{\rm g}$. Thus, a systematic investigation on gating effect of device B was conducted. A sketch of the field-effect device is shown in Fig.4(a). The gating voltage $V_{\rm g}$ is applied between the conducting 2DEG at the LAO/KTO interface and a silver paste electrode at the back of the KTO substrate. As shown in Fig.4(b), the carrier density of device B can be effectively tuned by $V_{\rm g}$. As $V_{\rm g}$ sweeps from +100 to 0 V, $n_{\rm S}$ decreases monotonically from 3.1×10^{13} to 2.1×10^{13} cm^{-2}, corresponding to the depletion of electrons caused by gating effect. It is worth noting that the relatively fast decrease in $n_{\rm S}$ is an indication of defect-induced localization and cannot be attributed to the change of $n_{\rm S}$ produced by the capacitance effect [29] (note that varying $V_{\rm g}$ between +100 and 0 V can induce a change of $n_{\rm S} \sim 5 \times 10^{12}$ cm^{-2} at most, which is only 50% of the experimentally observed value). Fig.4(c)

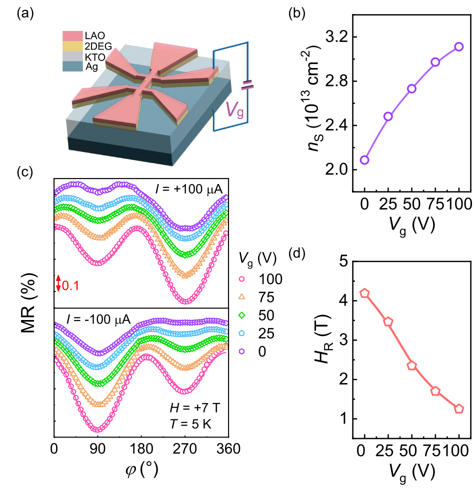

Fig. 4. (a) A sketch of the field-effect device. (b) Carrier density as a function of $V_{\rm g}$. (c) Angle dependence of MR measured under different $V_{\rm g}$. (d) Gate voltage dependence of the deduced Rashba field.

displays angle dependence of MR measured at various $V_{\rm g}$ with $I = \pm$ 300 μA and $H = +7$ T at 5 K. The MR curves are shifted vertically for clarity. As expected, the asymmetry between $\varphi = 90°$ and $\varphi = 270°$ of MR highly relies on the applied gate voltages. Reversing the current direction, the evolution process reverses. As displayed by the solid curves in Fig.4(c), the fits of Eqs. (1)-(3) show good agreement and correctly capture the features of the MR curves. The extracted values of $H_{\rm R}$ are summarized in Fig.4(d), indicating $H_{\rm R}$ significantly depends on $V_{\rm g}$. $H_{\rm R}$ monotonically increases as $V_{\rm g}$ varies from +100 to 0 V, and the magnitude of $H_{\rm R}$ increases more than three times from 1.3 T up to 4.2 T. Based on these data (Figs.4(b) and 4(d)), we can figure out the correspondence between the nonreciprocal charge transport and the gate-tunable carrier density, i.e., the nonreciprocal response is stronger as carrier density decreases. Remarkably, the giant tunability of current-induced Rashba field at the LAO/KTO interfaces provides a possibility to achieve electric field tunable two-terminal devices [30], [31].

V. Conclusion

We have demonstrated the nonreciprocal response for devices based on 2DEGs at the LAO/KTO interfaces. The BMR effect of our device has been clearly observed. Current induced Rashba field $H_{\rm R}$ is determined by analyzing angle-dependent MR, and we found that under the same applied current the device with the lower carrier density exhibits the higher $H_{\rm R}$. We further fabricate a field-effect device based on gating effect and realize the modulation of carrier density to further tune the nonreciprocal response. The magnitude of $H_{\rm R}$ varies by a factor of 3 from 1.3 T to 4.2 T when sweeping the gate voltage from +100 to 0 V. The highly tunable nonreciprocal response of conductive 2DEG at oxide interface in our study inspires a promising pathway towards realizing functional two-terminal spintronic devices.

References

[1] Y. Tokura and N. Nagaosa, “Nonreciprocal responses from non-centrosymmetric quantum materials,” *Nature Commun.*, vol. 9, no. 1, p. 3740, Sep. 2018, doi: 10.1038/s41467-018-05759-4.

Authorized licensed use limited to: INSTITUTE OF PHYSICS CAS. Downloaded on June 24,2024 at 03:10:16 UTC from IEEE Xplore. Restrictions apply.

[2] Y. Li, Y. Li, P. Li, B. Fang, X. Yang, Y. Wen, D.-X. Zheng, C.-H. Zhang, X. He, A. Manchon, Z.-H. Cheng, and X.-X. Zhang, "Nonreciprocal charge transport up to room temperature in bulk Rashba semiconductor α-GeTe," *Nature Commun.*, vol. 12, no. 1, p. 540, Jan. 2021, doi: 10.1038/s41467-020-20840-7.

[3] T. Guillet, C. Zucchetti, Q. Barbedienne, A. Marty, G. Isella, L. Cagnon, C. Vergnaud, H. Jaffrès, N. Reyren, J.-M. George, A. Fert, and M. Jamet, "Observation of large unidirectional Rashba magnetoresistance in Ge(111)," *Phys. Rev. Lett.*, vol. 124, no. 2, Jan. 2020, Art. no. 027201, doi: 10.1103/PhysRevLett.124.027201.

[4] A. Dyrdał, J. Barnał, and A. Fert, "Spin-momentum-locking inhomogeneities as a source of bilinear magnetoresistance in topological insulators," *Phys. Rev. Lett.*, vol. 124, no. 4, Jan. 2020, Art. no. 046802, doi: 10.1103/PhysRevLett.124.046802.

[5] R. Wakatsuki, Y. Saito, S. Hoshino, Y. M. Itahashi, T. Ideue, M. Ezawa, Y. Iwasa, and N. Nagaosa, "Nonreciprocal charge transport in noncentrosymmetric superconductors," *Sci. Adv.*, vol. 3, no. 4, Apr. 2017, Art. no. e1602390, doi: 10.1126/sciadv.1602390.

[6] T. Morimoto and N. Nagaosa, "Chiral anomaly and giant magnetochiral anisotropy in noncentrosymmetric weyl semimetals," *Phys. Rev. Lett.*, vol. 117, no. 14, Sep. 2016, Art. no. 146603, doi: 10.1103/PhysRevLett.117.146603.

[7] R. Wakatsuki and N. Nagaosa, "Nonreciprocal current in noncentrosymmetric Rashba superconductors," *Phys. Rev. Lett.*, vol. 121, no. 2, Jul. 2018, Art. no. 026601, doi: 10.1103/PhysRevLett.121.026601.

[8] L. M. Vicente-Arche, J. Bréhin, S. Varotto, M. Cosset-Cheneau, S. Mallik, R. Salazar, P. Noel, D. C. Vaz, F. Trier, S. Bhattacharya, A. Sander, P. Le Fèvre, F. Bertran, G. Saiz, G. Ménard, N. Bergeal, A. Barthélémy, H. Li, C. Lin, D. E. Nikonov, I. A. Young, J. E. Rault, L. Vila, J. Attané, and M. Bibes, "Spin–charge interconversion in $KTaO_3$ 2_D electron gases," *Adv. Mater.*, vol. 33, no. 43, Oct. 2021, Art. no. 2102102, doi: 10.1002/adma.202102102.

[9] P. He, S. M. Walker, S. S.-L. Zhang, F. Y. Bruno, M. S. Bahramy, J. M. Lee, R. Ramaswamy, K. Cai, O. Heinonen, G. Vignale, F. Baumberger, and H. Yang, "Observation of out-of-plane spin texture in a $SrTiO_3$(111) two-dimensional electron gas," *Phys. Rev. Lett.*, vol. 120, no. 26, Jun. 2018, Art. no. 266802, doi: 10.1103/PhysRevLett.120.266802.

[10] L. Miao, R. Du, Y. Yin, and Q. Li, "Anisotropic magneto-transport properties of electron gases at $SrTiO_3$(111) and (110) surfaces," *Appl. Phys. Lett.*, vol. 109, no. 26, Dec. 2016, Art. no. 261604, doi: 10.1063/1.4972985.

[11] P. He, S. S.-L. Zhang, D. Zhu, Y. Liu, Y. Wang, J. Yu, G. Vignale, and H. Yang, "Bilinear magnetoelectric resistance as a probe of three-dimensional spin texture in topological surface states," *Nature Phys.*, vol. 14, no. 5, pp. 495–499, May 2018, doi: 10.1038/s41567-017-0039-y.

[12] K. Yasuda, H. Yasuda, T. Liang, R. Yoshimi, A. Tsukazaki, K. S. Takahashi, N. Nagaosa, M. Kawasaki, and Y. Tokura, "Nonreciprocal charge transport at topological insulator/superconductor interface," *Nature Commun.*, vol. 10, no. 1, p. 2734, Jun. 2019, doi: 10.1038/s41467-019-10658-3.

[13] C. Ye, X. Xie, W. Lv, K. Huang, A. J. Yang, S. Jiang, X. Liu, D. Zhu, X. Qiu, M. Tong, T. Zhou, C.-H. Hsu, G. Chang, H. Lin, P. Li, K. Yang, Z. Wang, T. Jiang, and X. Renshaw Wang, "Nonreciprocal transport in a bilayer of $MnBi_2Te_4$ and pt," *Nano Lett.*, vol. 22, no. 3, pp. 1366–1373, Feb. 2022, doi: 10.1021/acs.nanolett.1c04756.

[14] G. Herranz, G. Singh, N. Bergeal, A. Jouan, J. Lesueur, J. Gázquez, M. Varela, M. Scigaj, N. Dix, F. Sánchez, and J. Fontcuberta, "Engineering two-dimensional superconductivity and Rashba spin–orbit coupling in $LaAlO_3/SrTiO_3$ quantum wells by selective orbital occupancy," *Nature Commun.*, vol. 6, no. 1, p. 6028, Jan. 2015, doi: 10.1038/ncomms7028.

[15] W. Niu, Y. Zhang, Y. Gan, D. V. Christensen, M. V. Soosten, E. J. Garcia-Suarez, A. Riisager, X. Wang, Y. Xu, R. Zhang, N. Pryds, and Y. Chen, "Giant tunability of the two-dimensional electron gas at the interface of γ-$Al_2O_3/SrTiO_3$," *Nano Lett.*, vol. 17, no. 11, pp. 6878–6885, Nov. 2017, doi: 10.1021/acs.nanolett.7b03209.

[16] A. Ohtomo and H. Y. Hwang, "A high-mobility electron gas at the $LaAlO_3/SrTiO_3$ heterointerface," *Nature*, vol. 427, no. 6973, pp. 423–426, Jan. 2004, doi: 10.1038/nature02308.

[17] A. D. Caviglia, M. Gabay, S. Gariglio, N. Reyren, C. Cancellieri, and J.-M. Triscone, "Tunable Rashba spin-orbit interaction at oxide interfaces," *Phys. Rev. Lett.*, vol. 104, no. 12, Mar. 2010, Art. no. 126803, doi: 10.1103/PhysRevLett.104.126803.

[18] D. C. Vaz, F. Trier, A. Dyrdał, A. Johansson, K. Garcia, A. Barthélémy, I. Mertig, J. Barnaś, A. Fert, and M. Bibes, "Determining the Rashba parameter from the bilinear magnetoresistance response in a two-dimensional electron gas," *Phys. Rev. Mater.*, vol. 4, no. 7, Jul. 2020, Art. no. 071001, doi: 10.1103/PhysRevMaterials.4.071001.

[19] J. Zhang, H. Zhang, X. Chen, J. Zhang, S. Qi, F. Han, Y. Chen, W. Zhao, F. Hu, B. Shen, and J. Sun, "Anisotropic bilinear magnetoresistance in (110) $SrTiO_3$-based two-dimensional electron gas," *Phys. Rev. B, Condens. Matter*, vol. 104, no. 4, Jul. 2021, Art. no. 045114, doi: 10.1103/PhysRevB.104.045114.

[20] C. O. Avci, K. Garello, A. Ghosh, M. Gabureac, S. F. Alvarado, and P. Gambardella, "Unidirectional spin Hall magnetoresistance in ferromagnet/normal metal bilayers," *Nature Phys.*, vol. 11, no. 7, pp. 570–575, Jul. 2015, doi: 10.1038/nphys3356.

[21] Y. Lv, J. Kally, D. Zhang, J. S. Lee, M. Jamali, N. Samarth, and J.-P. Wang, "Unidirectional spin-Hall and Rashba-edelstein magnetoresistance in topological insulator-ferromagnet layer heterostructures," *Nature Commun.*, vol. 9, no. 1, p. 111, Jan. 2018, doi: 10.1038/s41467-017-02491-3.

[22] D. Choe, M.-J. Jin, S.-I. Kim, H.-J. Choi, J. Jo, I. Oh, J. Park, H. Jin, H. C. Koo, B.-C. Min, S. Hong, H.-W. Lee, S.-H. Baek, and J.-W. Yoo, "Gate-tunable giant nonreciprocal charge transport in noncentrosymmetric oxide interfaces," *Nature Commun.*, vol. 10, no. 1, p. 4510, Oct. 2019, doi: 10.1038/s41467-019-12466-1.

[23] C. Zhang, X. Zhang, R. Xu, R. Liu, W. Niu, R. Gao, A. Song, W. Zhuang, Z. Chen, R. Zhang, and X. Wang, "Ion-liquid-gated $KTaO_3$-based electric double layer transistor," *IEEE Electron Device Lett.*, vol. 44, no. 12, pp. 1987–1990, Dec. 2023, doi: 10.1109/LED.2023.3322291.

[24] H. Zhang, H. Zhang, X. Yan, X. Zhang, Q. Zhang, J. Zhang, F. Han, L. Gu, B. Liu, Y. Chen, B. Shen, and J. Sun, "Highly mobile two-dimensional electron gases with a strong gating effect at the amorphous $LaAlO_3/KTaO_3$ interface," *ACS Appl. Mater. Interfaces*, vol. 9, no. 41, pp. 36456–36461, Oct. 2017, doi: 10.1021/acsami.7b12814.

[25] H. Uwe, T. Sakudo, and H. Yamaguchi, "Interband electronic Raman scattering in $SrTiO_3$," *Japanese J. Appl. Phys.*, vol. 24, no. S2, p. 519, Jan. 1985, doi: 10.7567/JJAPS.24S2.519.

[26] F. Y. Bruno, S. M. Walker, S. Riccó, A. de la Torre, Z. Wang, A. Tamai, T. K. Kim, M. Hoesch, M. S. Bahramy, and F. Baumberger, "Band structure and spin–orbital texture of the (111)-$KTaO_3$ 2D electron gas," *Adv. Electron. Mater.*, vol. 5, no. 5, May 2019, Art. no. 1800860, doi: 10.1002/aelm.201800860.

[27] H. Zhang, X. Yan, J. Zhang, J. Zhang, F. Han, H. Huang, S. Qi, W. Shi, B. Shen, and J. Sun, "The effect of fabrication conditions on 2DEGs transport characteristics at amorphous-$LaAlO_3/KTaO_3$ interfaces," *Mater. Res. Exp.*, vol. 6, no. 8, May 2019, Art. no. 086448, doi: 10.1088/2053-1591/ab240a.

[28] K. Narayanapillai, K. Gopinadhan, X. Qiu, A. Annadi, A. Ariando, T. Venkatesan, and H. Yang, "Current-driven spin orbit field in $LaAlO_3/SrTiO_3$ heterostructures," *Appl. Phys. Lett.*, vol. 105, no. 16, Oct. 2014, Art. no. 162405, doi: 10.1063/1.4899122.

[29] Z. Chen, Y. Liu, H. Zhang, Z. Liu, H. Tian, Y. Sun, M. Zhang, Y. Zhou, J. Sun, and Y. Xie, "Electric field control of superconductivity at the $LaAlO_3/KTaO_3$ (111) interface," *Science*, vol. 372, no. 6543, pp. 721–724, May 2021, doi: 10.1126/science.abb3848.

[30] Y. Yang, Y. Wu, and W. Wang, "Design of nonreciprocal multifunctional reflectionless bandpass filters by using circulators," *IEEE Trans. Circuits Syst. II, Exp. Briefs*, vol. 70, no. 1, pp. 106–110, Jan. 2023, doi: 10.1109/TCSII.2022.3208254.

[31] Z. Zhang, N. Wang, N. Cao, A. Wang, X. Zhou, K. Watanabe, T. Taniguchi, B. Yan, and W. Gao, "Controlled large non-reciprocal charge transport in an intrinsic magnetic topological insulator $MnBi_2Te_4$," *Nature Commun.*, vol. 13, no. 1, p. 6191, Oct. 2022, doi: 10.1038/s41467-022-33705-y.2022.6191.

Authorized licensed use limited to: INSTITUTE OF PHYSICS CAS. Downloaded on June 24,2024 at 03:10:16 UTC from IEEE Xplore. Restrictions apply.